Imaging of High Speed Gaseous Expansions through Varying Nozzle Geometries

A. S. Angle and H. R. Dunham

Angelo State University, Spring 2013
University Research Initiative

Imaging of High Speed Gaseous Expansions through Varying Nozzle Geometries

A. S. Angle, H.R. Dunham
Department of Physics and Geosciences
Angelo State University, San Angelo, Texas

Abstract

The goal of this experiment is to image SF_6 that is input into a vacuum from high pressure through a small nozzle. Interest is given to the dynamics of the bulk particle trajectories and distribution of velocities within the expansion plume. Imaging is accomplished via interferometry, where the measure of the fringe rate can be correlated to the gas density and pressure, ultimately revealing the velocity of the imaging location. Here we present the apparatus and discuss the measurements to be made.

Introduction

A nozzle is any passage or chamber through which a media passes. Specifically, within the field of thermodynamics, interest is placed on how a media's normal characteristics change with respect to a change in pressure, density, velocity, temperature, and/or entropy. The physics of nozzles was well established in the 1950s during the advances that were the beginning of the modern space-age; rockets and jet engines [1, 2]. Applications such as collimation of laser fluids, effusion of gas into thermodynamic chambers, generating atomic and molecular beams, and controlling thermal sources are now commonplace [3-6]. Current research in the field of nozzle physics focuses on supersonic flow characteristics and interactions on the atomic and molecular scale, such as in the observation of the interactions between different vapors and modeling the formation of atomic clusters and multi-nucleic collisions [7, 8]. Here, we report on the progress of an apparatus capable of imaging the supersonic expansion of a molecular gas through various nozzles. We employ a novel technique of imaging the expansion with a laser interferometer. By introducing a pressurized gas into a vacuum chamber, a large pressure differential and a high effusion speed can be expected. Through measurement of the interferometer fringe rate, we can relate the time changing index of refraction to the average velocity of a given position in the plume.

Experiment

Imaging of the plumes is accomplished using a 532 nm diode laser interferometer (Figure 1): the beam splitter is positioned such that one of the interferometer arms traverses the interior of a 3-axis vacuum chamber. The reference arm of the interferometer remains in air. The laser is first collimated with 2 converging lenses to ensure a focused beam and reduce the artifacts of the laser. The recombined arms then pass through a divergent lens to spread out the image of the interference fringes onto a screen for easy measurement of the fringe rate (Figure 2).

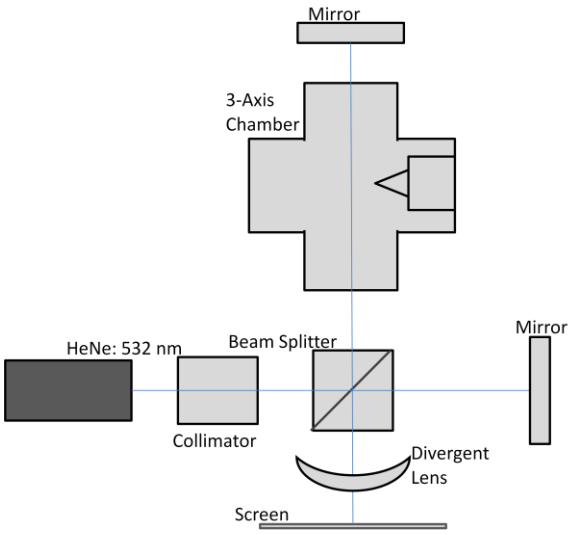

Figure 1: The interferometer setup for the apparatus.

The beam waist is 1.63 mm, much smaller than the plume, and therefore must interact with the plume at multiple positions to obtain a measurement of the velocity distribution for the bulk of the particles

entering the vacuum region. Initially we consider positions only axial with the nozzle port to measure plume fall off, varying the spacing by a fixed value, d (Figure 2).

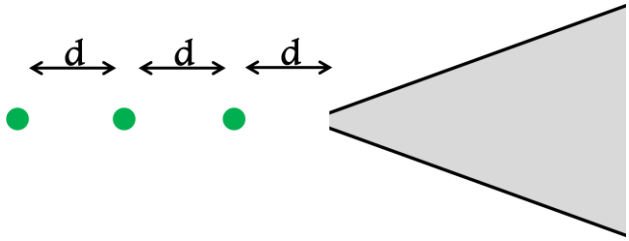

Figure 2: Scheme for obtaining bulk particle density inside the plume.

A high pressure differential is used to ensure a supersonic output at the nozzle. This is achieved using a pressurized gas input into a vacuum of approximately 10^{-6} Torr. With this high pressure differential, gas is introduced into several nozzle geometries: a 2.40 mm linear, a .035 mm conical, and a 1.64 mm trumpeted nozzle. All three are mounted onto a flange of the 3-axis chamber, and are interchangeable. Windows affixed to the other ports are used for alignment.

The gas inlet system involves a typical lecture bottle of SF_6 which, through a regulator, connects to a controlling needle valve at the chamber. The input gas diffuses through a small tube, of length 23.3 cm, before interacting with the nozzle.

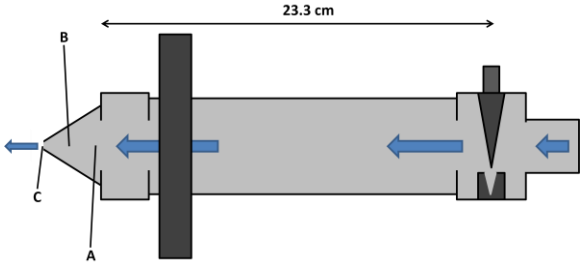

Figure 3: Needle valve and nozzle configuration. Point A represents the start of the nozzle, point B represents a point in the nozzle, and point C the end of the nozzle.

The procedure for obtaining data follows from the pressurization of the gas input system up to the needle gauge. Once the system has been taken down to vacuum, the needle gauge is opened by a specified amount and gas flows down the length of the tube. This results in a build-up of pressure in the nozzle to a maximum pressure, set by the regulator, and will correspond to a maximum density of the SF_6 plume. From this density change as the gas approaches the maximum value, the index of refraction will increase towards that of SF_6, n = 1.8, and the interference fringes will shift in response to the optical path length change. The fringe shift over the expansion time can be compared theoretically to obtain velocity.

Theory

Specifically, geometry of nozzles has a direct impact on the characteristics of the output gas: including velocity (Mach number), temperature, pressure, and density; all related in some form, whether explicitly or implicitly into the interaction by a continuity equation, Bernoulli's equation, for a compressible flow [9].

$$\rho_o u_o A_o = \rho u A \tag{1}$$

For gases in a polytropic expansion such as in this experiment, mass flow is conserved [9]. This has implications for the speed, u, density, ρ, and area, A, of the output gas.

The bulk flow behavior of the gas with respect to pressure, density, and temperature of the gas, are dependent on the adiabatic index or SF_6, γ = 1.093, and the velocity, Mach number, M, for a calorically perfect gas for an empirical system. This is justified as the input gas, SF_6, is 99.75% pure. The ratio of pressures at the entrance (Figure 3, A) to and a point (Figure 3, B) in the nozzle is defined as [9]:

$$\frac{P_o}{P} = \left(1 + \frac{\gamma-1}{2} M^2\right)^{\frac{\gamma}{\gamma-1}} \tag{2}$$

Similarly defined, the density, ρ, and temperature, T, ratios are written as:

$$\frac{\rho_o}{\rho} = \left(1 + \frac{\gamma-1}{2} M^2\right)^{\frac{1}{\gamma-1}} \tag{3}$$

$$\frac{T_o}{T} = 1 + \frac{\gamma-1}{2} M^2 \tag{4}$$

A changing density of gas causes a general change in index of refraction, n [5, 7] by:

$$n = 1 + k\frac{\rho}{\rho_{ref}} \tag{5}$$

Hence, a counting of the fringe rate will yield a change in the index of refraction that leads to a density at STP, ρ_{ref}, with respect to the density of the expanded gas through the constant k. This allows a measurement of velocity (Mach number) to be made using:

$$M(n) = \sqrt{\frac{2\left(\frac{k}{n-1}\right)^{\gamma-1} - 2}{\gamma - 1}} \tag{6}$$

Gas at this level of interaction will experience a general distribution or spread for their velocity or energy. Boltzmann statistics give a general model,

$$N(E) = N_o e^{-E/k_B T} \tag{7}$$

where E is the energy, T is temperature, k_B is the Boltzmann constant and can be equated to velocity, u, as:

$$N_o(u) = 4\pi u^2 \left(\frac{m}{2\pi k_B T}\right)^{3/2} e^{-mu^2/2k_B T} \tag{8}$$

We expect that exiting SF_6 will exhibit a Boltzmann distribution of velocities or kinetic energies (Figure 4).

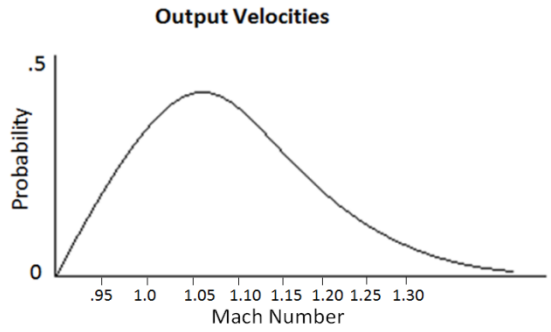

Figure 4: Generalized expected values for output velocities.

From this distribution the average, peak, and RMS speeds (u) can be calculated:

$$u_{avg} = \sqrt{8RT/\pi m} \tag{9}$$

$$u_{peak} = \sqrt{2RT/m} \tag{10}$$

$$u_{RMS} = \sqrt{3RT/m} \tag{11}$$

These equations will allow analysis of the bulk trajectories of particles of the output gas [10].

Under the current assumptions and theory, we predict to see velocities as a function of the index of refraction. Ultimately this can be related back to nozzle geometry using equations (1) and (5)

$$u(n) = \frac{k}{n-1}\left(\frac{A_o}{A}u_o\right) \tag{12}$$

where A_o is the area of the nozzle at the entrance and A is the area some distance into the nozzle.

Current Progress

Apparatus construction is completed and testing of vacuum integrity is finalized. The interferometer is assembled and was used to initially align the laser and image interference fringes. Progress is ongoing to image the SF_6 gas at different points within the plume, along the length and the edges of the expansion. The next goal is the optimization of the interferometer with respect to vibrational damping and alignment of the optical system. Once the system is aligned and damping is established, data collection with respect to fringe movement can be continued with acceptable RMS errors.

The regimes for pressure, density, and lighting were inadequate for the initial attempt at directly imaging the plume, forcing a different approach at imaging than had originally been envisioned. This led to the laser interferometer approach and a new host of obstacles, such as RMS vibrations from the building and the mechanical vacuum pump operation. This skews and distorts the images of the fringes, leading to incorrect values for the index, n. Our interferometer does not have an appropriate micrometer stage for systematic shifting of the beam splitter, a necessity for known beam positioning within the plume. The largest obstacles for this project during the last year were the limited time,

due to apparatus sharing, and availability and delay of apparatus parts. However, once the optical noise and alignment issues are resolved, data will be quickly forthcoming.

1) A. Balabel, Hegab, A.M., Nasr, M., El-Behery, S.M. *Assessment of Turbulence Modeling for Gas Flow in Two-Dimensional Convergent–Divergent Rocket Nozzle*, (Menoufiya University Press, Egypt, 2011), Vol. **35**, Iss. **7**, p 3408-3422.
2) Latvala, E.K., Anderson, T. P. *Studies of the Spreading of Rocket Exhaust Jets at High Altitudes*, (Northwest University Press, Illinois, 1961), Vol **4**, p 77-91.
3) Davies, M.G. *Thermal Sources and Fluid Flow*, (Building and Environment Magazine, 1988), Vol. **23**, Iss. **1**, p 25-28.
4) Facchini, B., Stecco, S.S. *Cooled Expansion in Gas Turbines*, (Energy and Conservation Management, 1999), Vol. **40**, Iss. **11**, p 1207-1224.
5) Mukhopadhyay, I., Singh, S. *Optically Pumped Far Infrared Molecular Lasers: Molecular and Application Aspects*, (Centre for Advanced Technology, India, 1997), Vol. **54**, Iss. **3**, p 395-410.
6) *Lasiris Dye Laser Product Manual*, (Stocker Yale, 2009), Version **12**, p 16-28.
7) Ramsey, N.F., *Thermal Beam Sources*, in *Atomic, Molecular and Optical Physics: Atoms and Molecules*, edited by R. Hulet, and F. B. Dunning (Academic Press, New York, 1996), Vol. **29B**, p 2.
8) Morse, M.D., *Supersonic Beam Sources*, in *Atomic, Molecular, and Optical Physics: Atoms and Molecules*, edited by R. Hulet, and F. B. Dunning (Academic Press, New York, 1996), Vol. **29B**, p 22.
9) Anderson, J.D., *Fundamentals of Aerodynamics*, 5th Ed. (McGraw Hill, New York, 2011), p 669.
10) F. Mandl, *Statistical Physics*,2nd Ed. (Manchester Physics, John Wiley & Sons, 2008) p 56.